Numer. Math. Theor. Meth. Appl.
doi: 10.4208/nmtma.2014.1316nm

Vol. 7, No. 1, pp. 23-40
February 2014

A Fitted Numerov Method for Singularly Perturbed Parabolic Partial Differential Equation with a Small Negative Shift Arising in Control Theory

R. Nageshwar Rao and P. Pramod Chakravarthy*

Department of Mathematics, Visvesvaraya National Institute of Technology, Nagpur, 440010, India.

Received 23 April 2013; Accepted (in revised version) 15 July 2013

Available online 24 January 2014

Abstract. In this paper, a fitted Numerov method is constructed for a class of singularly perturbed one-dimensional parabolic partial differential equations with a small negative shift in the temporal variable. Similar boundary value problems are associated with a furnace used to process a metal sheet in control theory. Here, the study focuses on the effect of shift on the boundary layer behavior of the solution via finite difference approach. When the shift parameter is smaller than the perturbation parameter, the shifted term is expanded in Taylor series and an exponentially fitted tridiagonal finite difference scheme is developed. The proposed finite difference scheme is unconditionally stable. When the shift parameter is larger than the perturbation parameter, a special type of mesh is used for the temporal variable so that the shift lies on the nodal points and an exponentially fitted scheme is developed. This scheme is also unconditionally stable. The applicability of the proposed methods is demonstrated by means of two examples.

AMS subject classifications: 65L11

Key words: Singular perturbations, parabolic partial differential equation, exponentially fitted method, differential-difference equations.

1. Introduction

Singularly perturbed partial differential equations are the equations in which the unknown function and its derivatives are evaluated at the same instance while in a singularly perturbed delay partial differential equation the past history is also taken into consideration while evaluating the unknown function and its derivatives. Such model problems occur from the modeling of biological, chemical, and physical systems which are characterized by both spatial and temporal variables and exhibit various spatio-temporal pat-

*Corresponding author. *Email addresses:* pramodpodila@yahoo.co.in (P. P. Chakravarthy), nrao_ragi@yahoo.co.in (R. N. Rao)

terns [1–5]. The mathematical model relating an automatically controlled furnace to process metal sheets [1] is given by the equation:

$$\frac{\partial u(x,t)}{\partial t} = D\frac{\partial^2 u(x,t)}{\partial x^2} + v(g(u(x,t-\tau)))\frac{\partial u(x,t)}{\partial x} + c[f(u(x,t-\tau)) - u(x,t)].$$

This equation is defined on a one-dimensional spatial domain $0 < x < 1$, where v is the instantaneous material strip velocity depending on a prescribed spatial average of the time-delayed temperature distribution $u(x,t-\tau)$, and f represents a distributed temperature source function depending on $u(x,t-\tau)$. The material strip to be heated is fed into the furnace by rollers whose speed is regulated by a speed controller. The furnace temperature is varied by means of a heater actuated by a heater controller. The control objective is to maintain a desired spatial temperature distribution in the incoming material within the furnace. This may be accomplished by placing temperature transducers along the material strip. A computer uses the information from the transducers to generate the appropriate control signals for the heater and feed-roller speed controllers. Owing to the possible presence of time delays in actuation, and in information transmission and processing, the controlled signals may be delayed in time.

Extensive literature has been developed over the last two decades on the singularly perturbed partial differential equations [6–17], but the theory and numerical solutions of singularly perturbed delay partial differential equations are still at the initial stage. Ansari et al. [18] in their work considered a Dirichlet boundary value problem of singularly perturbed delay parabolic partial differential equation. A numerical method comprising a standard finite difference operator on a rectangular piecewise uniform fitted mesh of $N_x \times N_t$ elements condensing in the boundary layers is developed. The method is proved to be robust with respect to the small parameter. Yulan Wang [19] considered a similar type of singularly perturbed delay parabolic partial differential equation wherein the domain is divided into three sub-domains namely the two inner regions and an outer region and a reliable analytical technique is developed. Bashier and Patidar [20] developed a robust fitted operator finite difference method for the numerical solution of a singularly perturbed delay parabolic partial differential equation. Sufficient analysis is carried out to verify the validity of the solutions obtained.

In this paper, we presented exponentially fitted finite difference methods for a class of singularly perturbed one-dimensional parabolic partial differential equations with a small negative shift in the temporal variable. Briefly, the outline is as follows: In Section 2, we state the problem. In Section 2.2, the finite difference method is developed considering the shift parameter to be smaller than the perturbation parameter, the truncation error in the finite difference scheme is calculated and stability analysis is carried out. In Section 2.4, the shift parameter is considered to be larger than the perturbation parameter and the finite difference method is developed. The truncation error is calculated and stability analysis is carried out. To demonstrate the efficiency of the proposed methods, numerical experiments are carried out for two test problems and the results are given in Section 3. Finally the conclusions are given in the last section.

2. Statement of the problem

In this paper, we consider a class of singularly perturbed parabolic partial differential equations with a small negative shift, of the form:

$$\frac{\partial u(x,t)}{\partial t} - \epsilon \frac{\partial^2 u(x,t)}{\partial x^2} + a(x,t)u(x,t) + b(x,t)u(x,t-\delta) = f(x,t), \tag{2.1}$$

$(x,t) \in D : \{0 < x < 1, 0 < t \leq T\}$ with the initial data

$$u(x,t) = \alpha(x,t), \quad (x,t) \in D_1 : \{0 \leq x \leq 1, -\delta \leq t \leq 0\} \tag{2.2a}$$

and the boundary conditions

$$u(0,t) = \phi(t), \qquad 0 < t \leq T, \tag{2.2b}$$
$$u(1,t) = \psi(t), \qquad 0 < t \leq T, \tag{2.2c}$$

where $0 < \epsilon \ll 1$ is the singular perturbation parameter, $\delta > 0$ represents the small shift parameter, $a(x,t)$, $b(x,t)$, $f(x,t)$, $\alpha(x,t)$, $\phi(t)$, $\psi(t)$ are sufficiently smooth and bounded functions.

We impose the compatibility condition on the initial function $\alpha(x,t)$:

$$\alpha(0,0) = \phi(0), \qquad \alpha(1,0) = \psi(0),$$
$$\frac{\partial \phi(0)}{\partial t} - \epsilon \frac{\partial^2 \alpha(0,0)}{\partial x^2} + a(0,0)\alpha(0,0) + b(0,0)\alpha(0,-\delta) = f(0,0),$$

and

$$\frac{\partial \psi(0)}{\partial t} - \epsilon \frac{\partial^2 \alpha(1,0)}{\partial x^2} + a(1,0)\alpha(1,0) + b(1,0)\alpha(1,1-\delta) = f(1,0).$$

Under the above assumptions and conditions, problem (2.1) with the initial data (2.2a) and the boundary conditions (2.2b)-(2.2c) has a unique solution [18].

2.1. When the shift parameter is smaller than the singular perturbation parameter

When the shift parameter δ is smaller than the perturbation parameter ϵ, the use of Taylor's series expansion for the shifted term is valid [21]. Hence the Taylor series approximation for the shifted term is taken as follows:

$$u(x,t-\delta) \approx u(x,t) - \delta \frac{\partial u(x,t)}{\partial t} + \mathcal{O}(\delta^2). \tag{2.3}$$

Substituting Eq. (2.3) in Eq. (2.1)we get

$$[1 - b(x,t)\delta]\frac{\partial u(x,t)}{\partial t} + [a(x,t) + b(x,t)]u(x,t) = f(x,t) + \epsilon \frac{\partial^2 u(x,t)}{\partial x^2} \tag{2.4}$$

subject to the conditions

$$u(x,0) = \alpha(x,0), \qquad 0 \le x \le 1, \tag{2.5a}$$
$$u(0,t) = \phi(t), \qquad 0 < t \le T, \tag{2.5b}$$
$$u(1,t) = \psi(t), \qquad 0 < t \le T. \tag{2.5c}$$

Since the shift parameter δ is assumed to be smaller than ϵ, (2.4)-(2.5) will be a good approximation to the problem (2.1)-(2.2).

2.2. Fitted Numerov method

To describe the method, we consider the linear singularly perturbed delay parabolic partial differential equation (2.4) subject to the conditions (2.5). Now we divide the time interval $[0,T]$ into N equal parts with constant step size Δt. Let $0 = t_0, t_1, \cdots, t_N = T$ be the mesh points. Then we have $t_n = n\Delta t$, $n = 0,1,2,\cdots,N$.

Applying Backward Euler formula for time derivative in Eq. (2.4) we obtain a linear ordinary differential equation at each time step as

$$\begin{aligned}&[1 - b(x,t_n)\delta]\frac{(U^n - U^{n-1})}{\Delta t} + [a(x,t_n) + b(x,t_n)]U^n \\ =&f(x,t_n) + \epsilon\frac{d^2U^n}{dx^2}, \quad 0 < x < 1,\end{aligned} \tag{2.6}$$

where $U^n = U(x,t_n) \approx u(x,t_n)$, $n = 1,2,\cdots,N$. The above Eq. (2.6) can be rewritten as

$$-\epsilon\frac{d^2U}{dx^2} + P(x)U(x) = Q(x), \tag{2.7}$$

where

$$\begin{aligned}&U = U^n, \quad P(x) = \frac{1}{\Delta t} + \Big(1 - \frac{\delta}{\Delta t}\Big)b(x,t_n) + a(x,t_n),\\ &Q(x) = f(x,t_n) + \Big(\frac{1 - b(x,t_n)\delta}{\Delta t}\Big)U^{n-1}(x),\\ &P(x) = P(x,t_n), \quad Q(x) = Q(x,t_n), \quad x \in [0,1].\end{aligned}$$

The boundary conditions (2.5) can be written as

$$U(x,0) = \alpha(x,0), \qquad x \in [0,1], \tag{2.8a}$$
$$U(0) = U(0,t_n) = \phi^n = \phi(t_n), \qquad n = 1,2,\cdots,N, \tag{2.8b}$$
$$U(1) = U(1,t_n) = \psi^n = \psi(t_n), \qquad n = 1,2,\cdots,N. \tag{2.8c}$$

The solution to the reduced problem of (2.7) is

$$U_0(x) = \frac{Q(x)}{P(x)} \tag{2.9}$$

and it does not satisfy both the boundary conditions of (2.8b)-(2.8c).

The solution of Eq. (2.7) is of the form

$$U(x) = U_0 + V_0 + W_0, \tag{2.10}$$

where V_0 is the left boundary layer function (or solution) and W_0 is the right boundary layer function (or solution) and they satisfy the equations

$$-\frac{d^2V_0}{d\tau^2} + P(0)V_0 = 0, \tag{2.11a}$$

$$-\frac{d^2W_0}{d\xi^2} + P(1)W_0 = 0, \tag{2.11b}$$

with

$$V_0(\tau = 0) + W_0(\xi = 1/\sqrt{\epsilon}) = \phi^n - U_0(0), \tag{2.12a}$$

$$V_0(\tau = 1/\sqrt{\epsilon}) + W_0(\xi = 0) = \psi^n - U_0(1), \tag{2.12b}$$

$$V_0(\tau = \infty) + W_0(\xi = \infty) = 0, \tag{2.12c}$$

where $\tau = x/\sqrt{\epsilon}$ and $\xi = (1-x)/\sqrt{\epsilon}$, the stretching transformations for the boundary layers.

Solving Eqs. (2.11a) and (2.11b) we get

$$V_0(\tau) = Ae^{-\sqrt{P(0)}\tau}, \tag{2.13a}$$

$$W_0(\tau) = Be^{-\sqrt{P(1)}\xi}, \tag{2.13b}$$

where A and B are given by

$$A = \frac{(\phi^n - U_0^n(0)) - (\psi^n - U_0^n(1))\exp\left(-\sqrt{\frac{P(1)}{\epsilon}}\right)}{1 - \exp\left(-\frac{\sqrt{P(0)}+\sqrt{P(1)}}{\sqrt{\epsilon}}\right)},$$

$$B = \frac{(\psi^n - U_0^n(1)) - (\phi^n - U_0^n(0))\exp\left(-\sqrt{\frac{P(0)}{\epsilon}}\right)}{1 - \exp\left(-\frac{\sqrt{P(0)}+\sqrt{P(1)}}{\sqrt{\epsilon}}\right)}.$$

We rewrite Eq. (2.7) as

$$\epsilon\frac{d^2U}{dx^2} = P(x)U(x) - Q(x) = g(x,U). \tag{2.14}$$

Now the spatial domain $[0,1]$ is divided into M equal parts with constant mesh length h. Let $0 = x_0, x_1, \cdots, x_{r-1}, x_r, x_{r+1}, \cdots, x_M = 1$ be the mesh points such that $x_m = mh$, $m = 0, 1, 2, \cdots, M$ and $r = M/2$, $x_r = 1/2$. In the interval $[0, 1/2]$ the boundary layer will be in the left hand side, i.e., at $x = 0$ and in the interval $[1/2, 1]$, the boundary layer will be in the right hand side, i.e., at $x = 1$.

At $x = x_m$, the above differential equation (2.14) can be written as

$$\epsilon U_m'' = g(x_m, U_m),$$

where $g(x_m, U_m) = P(x_m)U_m - Q(x_m)$ or $g_m = P_m U_m - Q_m$, $P_m = P(x_m)$, $Q_m = Q(x_m)$, $g_m = g(x_m, U_m)$.

By Numerov method we have,

$$\epsilon\Big(\frac{U_{m-1} - 2U_m + U_{m+1}}{h^2}\Big) = \frac{1}{12}(g_{m-1} + 10g_m + g_{m+1}),$$

i.e.,

$$\begin{aligned}&\frac{\epsilon}{h^2}(U_{m-1} - 2U_m + U_{m+1}) - \frac{1}{12}(P_{m-1}U_{m-1} + 10P_mU_m + P_{m+1}U_{m+1})\\ &= -\frac{1}{12}(Q_{m-1} + 10Q_m + Q_{m+1}), \quad m = 1, 2, \cdots, r-1. \end{aligned} \tag{2.15}$$

In the interval $[0, 1/2]$, we introduce a fitting factor σ in the above scheme and is obtained from the theory of singular perturbations as follows:

$$\begin{aligned}&\frac{\epsilon}{h^2}\sigma(U_{m-1} - 2U_m + U_{m+1}) - \frac{1}{12}(P_{m-1}U_{m-1} + 10P_mU_m + P_{m+1}U_{m+1})\\ &= -\frac{1}{12}(Q_{m-1} + 10Q_m + Q_{m+1}), \quad m = 1, 2, \cdots, r-1.\end{aligned}$$

The difference scheme can be rewritten as

$$\begin{aligned}&\Big(\frac{\epsilon\sigma}{h^2} - \frac{1}{12}P_{m-1}\Big)U_{m-1} - \Big(\frac{2\epsilon\sigma}{h^2} + \frac{5}{6}P_m\Big)U_m + \Big(\frac{\epsilon\sigma}{h^2} - \frac{1}{12}P_{m+1}\Big)U_{m+1}\\ &= -\frac{1}{12}(Q_{m-1} + 10Q_m + Q_{m+1}), \quad m = 1, 2, \cdots, r-1.\end{aligned} \tag{2.16}$$

We find the fitting factor σ in such a way that the solution of (2.16) converges to the solution of (2.7). As $h \to 0$, Eq. (2.16) reduces to

$$\frac{\sigma}{\rho^2}(U_{m-1} - 2U_m + U_{m+1}) = \frac{1}{12}P(0)(U_{m-1} + 10U_m + U_{m+1}), \tag{2.17}$$

where $\rho = h/\sqrt{\epsilon}$. Substituting (2.13a) in (2.17) and simplifying, we get the fitting factor as

$$\sigma(\rho) = \frac{\rho^2 P(0)\Big(e^{\sqrt{P(0)}\rho} + 10 + e^{-\sqrt{P(0)}\rho}\Big)}{48\sinh^2\Big(\frac{\sqrt{P(0)}\rho}{2}\Big)}. \tag{2.18}$$

This will be the fitting factor in the interval $[0, 1/2]$.

We solve the tridiagonal system (2.16) subject to the fitting factor (2.18) by using Thomas algorithm for each time step. The value of $U_r = U(x = 1/2)$ is obtained by the solution of the reduced problem. i.e., $U_0(x)$.

In the interval $[1/2,1]$ the boundary layer will be in the right hand side, i.e., at $x=1$. We introduce the fitting factor σ_1 in the difference scheme (2.15) as

$$\begin{aligned}&\frac{\epsilon}{h^2}\sigma_1(U_{m-1}-2U_m+U_{m+1})-\frac{1}{12}(P_{m-1}U_{m-1}+10P_mU_m+P_{m+1}U_{m+1})\\&=-\frac{1}{12}(Q_{m-1}+10Q_m+Q_{m+1}),\quad m=r+1,r+2,\cdots,M-1.\end{aligned}$$

The above scheme can be rewritten as

$$\begin{aligned}&\Big(\frac{\epsilon\sigma_1}{h^2}-\frac{1}{12}P_{m-1}\Big)U_{m-1}-\Big(\frac{2\epsilon\sigma_1}{h^2}+\frac{5}{6}P_m\Big)U_m+\Big(\frac{\epsilon\sigma_1}{h^2}-\frac{1}{12}P_{m+1}\Big)U_{m+1}\\&=-\frac{1}{12}(Q_{m-1}+10Q_m+Q_{m+1}),\quad m=r+1,r+2,\cdots,M-1.\end{aligned}\tag{2.19}$$

We find the fitting factor σ_1 in such a way that the solution of (2.19) converges to the solution of (2.7). As $h\to 0$, Eq. (2.19) reduces to

$$\frac{\sigma_1}{\rho^2}(U_{m-1}-2U_m+U_{m+1})=\frac{1}{12}P(1)(U_{m-1}+10U_m+U_{m+1}),\tag{2.20}$$

where $\rho=h/\sqrt{\epsilon}$. Substituting (2.13b) in (2.20) and simplifying, we get the fitting factor as

$$\sigma_1(\rho)=\frac{\rho^2P(1)\Big(e^{\sqrt{P(1)}\rho}+10+e^{-\sqrt{P(1)}\rho}\Big)}{48\sinh^2\Big(\frac{\sqrt{P(1)}\rho}{2}\Big)}.\tag{2.21}$$

This will be the fitting factor in the interval $[1/2,1]$. We solve the tridiagonal system (2.19) subject to the fitting factor (2.21) by using Thomas algorithm for each time step.

Remark 2.1. *When*

$$P(0)=P(1),$$

both the fitting factors become equal and the constant fitting factor is

$$\sigma(\rho)=\frac{\rho^2P(0)\Big(e^{\sqrt{P(0)}\rho}+10+e^{-\sqrt{P(0)}\rho}\Big)}{48\sinh^2\Big(\frac{\sqrt{P(0)}\rho}{2}\Big)}.$$

2.3. Truncation error and stability analysis

Eq. (2.16) can be written as

$$\begin{aligned}&\Big(\frac{\epsilon\sigma}{h^2}-\frac{1}{12\Delta t}-\frac{1}{12}b(x_{m-1},t_n)+\frac{\delta}{12\Delta t}b(x_{m-1},t_n)-\frac{1}{12}a(x_{m-1},t_n)\Big)U^n_{m-1}\\&-\Big(\frac{2\epsilon\sigma}{h^2}+\frac{5}{6\Delta t}+\frac{5}{6}b(x_m,t_n)-\frac{5\delta}{6\Delta t}b(x_m,t_n)+\frac{5}{6}a(x_m,t_n)\Big)U^n_m\\&+\Big(\frac{\epsilon\sigma}{h^2}-\frac{1}{12\Delta t}-\frac{1}{12}b(x_{m+1},t_n)+\frac{\delta}{12\Delta t}b(x_{m+1},t_n)-\frac{1}{12}a(x_{m+1},t_n)\Big)U^n_{m+1}\end{aligned}$$

$$= -\frac{1}{12}(f(x_{m-1},t_n)+10f(x_m,t_n)+f(x_{m+1},t_n)) - \frac{1}{12\Delta t}(1-b(x_{m-1},t_n)\delta)U_{m-1}^{n-1}$$
$$-\frac{5}{6\Delta t}(1-b(x_m,t_n)\delta)U_m^{n-1} - \frac{1}{12\Delta t}(1-b(x_{m+1},t_n)\delta)U_{m+1}^{n-1}. \tag{2.22}$$

Multiplying Eq. (2.16) by $h^2\Delta t$ we obtain

$$\Big(\epsilon\sigma\Delta t - \frac{h^2}{12} - \frac{h^2\Delta t}{12}b(x_{m-1},t_n) + \frac{h^2\delta}{12}b(x_{m-1},t_n) - \frac{h^2\Delta t}{12}a(x_{m-1},t_n)\Big)U_{m-1}^n$$
$$-\Big(2\epsilon\sigma\Delta t + \frac{5}{6}h^2 + \frac{5}{6}h^2\Delta t\, b(x_m,t_n) - \frac{5}{6}h^2\delta\, b(x_m,t_n) + \frac{5}{6}h^2\Delta t a(x_m,t_n)\Big)U_m^n$$
$$+\Big(\epsilon\sigma\Delta t - \frac{h^2}{12} - \frac{h^2\Delta t}{12}b(x_{m+1},t_n) + \frac{h^2\delta}{12}b(x_{m+1},t_n) - \frac{h^2\Delta t}{12}a(x_{m+1},t_n)\Big)U_{m+1}^n$$
$$= -\frac{h^2\Delta t}{12}(f(x_{m-1},t_n)+10f(x_m,t_n)+f(x_{m+1},t_n)) - \frac{h^2}{12}(1-b(x_{m-1},t_n)\delta)U_{m-1}^{n-1}$$
$$-\frac{5h^2}{6}(1-b(x_m,t_n)\delta)U_m^{n-1} - \frac{h^2}{12}(1-b(x_{m+1},t_n)\delta)U_{m+1}^{n-1}. \tag{2.23}$$

Let $F_m^n(U) = 0$ represent the difference equation (2.23) approximating the partial differential equation (2.4) at the mesh point (x_m, t_n) and the exact solution of the partial differential equation (2.4) be denoted by $u(x,t)$. Replacing U with u at the mesh points of the differential equation, we get

$$T_m^n = F(u)$$
$$=\Big(\epsilon\sigma\Delta t - \frac{h^2}{12} - \frac{h^2\Delta t}{12}b(x_{m-1},t_n) + \frac{h^2\delta}{12}b(x_{m-1},t_n) - \frac{h^2\Delta t}{12}a(x_{m-1},t_n)\Big)u_{m-1}^n$$
$$-\Big(2\epsilon\sigma\Delta t + \frac{5}{6}h^2 + \frac{5}{6}h^2\Delta t\, b(x_m,t_n) - \frac{5}{6}h^2\delta\, b(x_m,t_n) + \frac{5}{6}h^2\Delta t a(x_m,t_n)\Big)u_m^n$$
$$+\Big(\epsilon\sigma\Delta t - \frac{h^2}{12} - \frac{h^2\Delta t}{12}b(x_{m+1},t_n) + \frac{h^2\delta}{12}b(x_{m+1},t_n) - \frac{h^2\Delta t}{12}a(x_{m+1},t_n)\Big)u_{m+1}^n$$
$$+\frac{h^2\Delta t}{12}(f(x_{m-1},t_n)+10f(x_m,t_n)+f(x_{m+1},t_n)) + \frac{h^2}{12}(1-b(x_{m-1},t_n)\delta)u_{m-1}^{n-1}$$
$$+\frac{5}{6}(1-b(x_m,t_n)\delta)u_m^{n-1} + \frac{h^2}{12}(1-b(x_{m+1},t_n)\delta)u_{m+1}^{n-1}, \tag{2.24}$$

where T_m^n denotes the local truncation error at the mesh point (x_m, t_n).

By using the Taylor's series expansions in (2.24) and using the Eq. (2.4), we get the principal part of T_m^n as

$$T_m^n = \Big(\frac{h^3\Delta t}{12}[b(x_{m-1},t_n) - b(x_{m+1},t_n) + a(x_{m-1},t_n) - a(x_{m+1},t_n)]\Big)\frac{\partial u}{\partial x}\Big|_m^n.$$

Hence

$$T_m^n = \mathcal{O}(h^3\Delta t). \tag{2.25}$$

Multiplying Eq. (2.22) by Δt and taking $\lambda = \Delta t/h^2$, we obtain

$$\begin{aligned}
&\Big(\epsilon\delta\lambda - \frac{1}{12} - \frac{1}{12}(\Delta t - \delta)b(x_{m-1}, t_n) - \frac{\Delta t}{12}a(x_{m-1}, t_n)\Big)U^n_{m-1} \\
&\quad - \Big(2\epsilon\delta\lambda + \frac{5}{6} + \frac{5}{6}(\Delta t - \delta)b(x_m, t_n) + \frac{5}{6}a(x_{m-1}, t_n)\Big)U^n_m \\
&\quad + \Big(\epsilon\delta\lambda - \frac{1}{12} - \frac{1}{12}(\Delta t - \delta)b(x_{m+1}, t_n) - \frac{\Delta t}{12}a(x_{m+1}, t_n)\Big)U^n_{m+1} \\
&= -\frac{\Delta t}{12}(f(x_{m-1}, t_n) + 10f(x_m, t_n) + f(x_{m+1}, t_n)) - \frac{1}{12}(1 - b(x_{m-1}, t_n)\delta)U^{n-1}_{m-1} \\
&\quad - \frac{5}{6}(1 - b(x_m, t_n)\delta)U^{n-1}_m - \frac{1}{12}(1 - b(x_{m+1}, t_n)\delta)U^{n-1}_{m+1}. \qquad (2.26)
\end{aligned}$$

As $\Delta t \to 0$ we get

$$\begin{aligned}
&\Big(\epsilon\delta\lambda - \frac{1}{12} + \frac{\delta}{12}b(x_{m-1}, t_n)\Big)U^n_{m-1} - \Big(2\epsilon\delta\lambda + \frac{5}{6} - \frac{5\delta}{6}b(x_m, t_n)\Big)U^m_n \\
&\quad + \Big(\epsilon\delta\lambda - \frac{1}{12} + \frac{\delta}{12}b(x_{m+1}, t_n)\Big)U^n_{m+1} \\
&= -\frac{1}{12}(U^{n-1}_{m-1} + 10U^{n-1}_m + U^{n-1}_{m+1}) + \frac{\delta}{12}(b(x_{m-1}, t_n)U^{n-1}_{m-1} \\
&\quad + 10b(x_m, t_n)U^{n-1}_m + b(x_{m+1}, t_n)U^{n-1}_{m+1}). \qquad (2.27)
\end{aligned}$$

To study the Von Neumann linear stability [4, 23], we assume that there exists an error $e^n_m = \xi^n e^{i\beta mh}$ at each grid point (x_m, t_n) where the phase angle β is real, $i = \sqrt{-1}$ and ξ is the amplitude and may be complex.

Substituting $e^n_m = \xi^n e^{i\beta mh}$ in Eq. (2.27) and simplifying we get

$$\xi = \frac{\{(e^{-i\beta h} + 10 + e^{i\beta h}) - 12\delta\theta\}}{\{(e^{-i\beta h} + 10 + e^{i\beta h}) - \delta\theta\} + 48\epsilon\sigma\lambda\sin^2\left(\frac{\beta h}{2}\right)},$$

where $\theta = b(x_{m-1}, t_n)e^{-i\beta h} + 10b(x_m, t_n) + b(x_{m+1}, t_n)e^{i\beta h}$.

As the parameters ϵ and δ are very small quantities, it can be observed that $|\xi| \leq 1$. For stability, the amplification factor ξ has to satisfy the condition $|\xi| \leq 1$ for all $-\pi \leq \beta \leq \pi$. Hence the scheme (2.16) or (2.19) is unconditionally stable.

2.4. When the delay parameter is larger than singular perturbation parameter

When the delay parameter δ is larger than the perturbation parameter ϵ, use of Taylor's series expansion for the terms containing delay in (2.1) is not valid and hence the numerical method presented in the previous section fails. In this section we present a numerical scheme which works nicely when the delay parameter is larger than perturbation parameter also. To describe the method, we consider the linear singularly perturbed parabolic partial differential equation (2.1) subject to the initial and boundary conditions (2.2).

Let the time interval $[0,T]$ be partitioned into N equal parts with constant step size Δt. We choose the step size Δt in such a way that the shift parameter $\delta = s\Delta t$, where s is some positive integer.

Let $0 = t_0, t_1, \cdots, t_N = T$ be the mesh points. Then we have $t_n = nT/N = n\Delta t$, $n = 0, 1, \cdots, N$.

Applying Backward Euler formula for time derivative in Eq. (2.1) we obtain

$$\begin{aligned}&\frac{u^n - u^{n-1}}{\Delta t} + a(x,t_n)u^n(x) + b(x,t_n)u^{n-s}(x)\\ =&\epsilon\frac{d^2u^n}{dx^2} + f^n(x), \quad n = 0,1,2,\cdots,N,\end{aligned} \tag{2.28}$$

where $u^n = u(x,t_n)$, $f^n(x) = f(x,t_n)$.

For each time step, the above equation is an ordinary differential equation which can be rewritten as

$$-\epsilon\frac{d^2u}{dx^2} + P(x)u(x) = Q(x), \tag{2.29}$$

where

$$P(x) = \alpha(x,t_n) + \frac{1}{\Delta t}, \quad Q(x) = f^n(x) + \frac{1}{\Delta t}u^{n-1} - b(x,t_n)u^{n-s},$$

subject to the conditions

$$u(0) = u^n(0) = \phi(t_n), \quad n = 1,2,\cdots,r, \tag{2.30a}$$

$$u(1) = u^n(1) = \psi(t_n), \quad n = 1,2,\cdots,r, \tag{2.30b}$$

$$u(x,t_n) = \alpha(x,t_n), \quad x \in [0,1], \quad n = -s, -s+1, \cdots, 0. \tag{2.30c}$$

By using the initial data, we can rewrite

$$Q(x) = \begin{cases} f^n(x) + \dfrac{1}{\Delta t}u^{n-1} - b(x,t_n)\alpha(x,t_{n-s}), & \text{for } n = 0,1,2,\cdots,s,\\ f^n(x) + \dfrac{1}{\Delta t}u^{n-1} - b(x,t_n)u^{n-s}, & \text{for } n = s+1, s+2, \cdots, N. \end{cases}$$

Using this in (2.29) and the fitted Numerov method described in Section 2.2 and the boundary conditions given in (2.30), we get the solution at each time step.

2.5. Truncation error and stability analysis

Using the procedure described in Section 2.3, it has been observed that the principal part of truncation error is given by

$$T_m^n = \Big(\frac{h^3\Delta t}{12}[a(x_{m-1},t_n) - a(x_{m+1},t_n)]\Big)\frac{\partial u}{\partial x}\Big|_m^n.$$

Hence $T_m^n = \mathcal{O}(h^3\Delta t)$.

Using Von Neumann linear stability described in Section 2.3, it has been observed that the amplification factor ξ is given by

$$\xi = \frac{\left[e^{-i\beta h} + 10 + e^{i\beta h}\right]}{\left[e^{-i\beta h} + 10 + e^{i\beta h}\right] + 48\epsilon\sigma\lambda \sin^2\left(\frac{\beta h}{2}\right)}.$$

We find that the amplification factor ξ satisfies the condition $|\xi| \leq 1$ for all $-\pi \leq \beta \leq \pi$. Hence the proposed scheme is unconditionally stable.

3. Numerical results

To demonstrate the applicability of the methods presented above, we consider two problems of singularly perturbed parabolic partial differential equations with shift parameter δ less than the perturbation parameter ϵ. Since the exact solutions of the problems for various values of δ are not known, the maximum point wise error for the examples are calculated using the following double mesh principle [22]

$$E_\epsilon^{M,N} = \max_{0\leq i\leq N} \left|U_i^{M,N} - U_i^{2M,2N}\right|,$$

where U^M, N_ϵ is the numerical solution obtained on a mesh containing M points in the spatial direction and N points in the temporal direction whereas $U_i^{2M,2N}$ is the numerical solution obtained on a mesh containing $2M$ points in the spatial direction and $2N$ points in the temporal direction.

The numerical rate of convergence for all the examples has been calculated by the formula

$$R^{M,N} = \frac{\log\left|E_\epsilon^{M,N}/E_\epsilon^{2M,2N}\right|}{\log 2}.$$

Example 3.1. For

$$\frac{\partial u(x,t)}{\partial t} - \epsilon\frac{\partial^2 u(x,t)}{\partial x^2} + \frac{(1+x^2)}{2}u(x,t) + u(x,t-\delta) = t^3,$$
$$(x,t) \in D : \{0 < x < 1, 0 < t \leq 2\},$$

with the initial data

$$u(x,t) = 0, \quad (x,t) \in D_1 : \{0 \leq x \leq 1, -\delta \leq t \leq 0\}$$

and the boundary conditions $u(0,t) = 0$ and $u(1,t) = 0$.

The maximum absolute errors are tabulated in the form of Table 1 for $\delta = 0.5\epsilon$ with various values of ϵ. The graph of the solution for $\epsilon = 2^{-20}$ and $\delta = 0.5\epsilon$ is plotted in Fig. 1 to examine the effect of small shift on the boundary layer behavior of the solution. The maximum absolute errors with $\epsilon = 0.01$ and for various values of δ are tabulated in Table 2. The graph of the solution for $\epsilon = 2^{-10}$ and $\delta = 0.06$ is plotted in Fig. 2 to examine

Table 1: The maximum point wise errors and numerical rates of convergence for Example 3.1 with $\delta = 0.5\epsilon$.

	$M \rightarrow$	64	128	256	512	1024
$\epsilon \downarrow$	$N \rightarrow$	20	40	80	160	320
2^{-1}		4.5965e-002	2.3365e-002	1.1780e-002	5.9146e-003	2.9635e-003
		0.9762	0.9880	0.9940	0.9970	0.9985
2^{-2}		4.8072e-002	2.4416e-002	1.2304e-002	6.1765e-003	3.0944e-003
		0.9774	0.9886	0.9943	0.9971	0.9986
2^{-4}		4.9092e-002	2.4914e-002	1.2550e-002	6.2989e-003	3.1553e-003
		0.9785	0.9892	0.9946	0.9973	0.9986
2^{-6}		4.9913e-002	2.5333e-002	1.2763e-002	6.4055e-003	3.2088e-003
		0.9784	0.9891	0.9945	0.9973	0.9986
2^{-8}		5.2462e-002	2.6615e-002	1.3405e-002	6.7272e-003	3.3697e-003
		0.9790	0.9895	0.9947	0.9974	0.9987
2^{-10}		5.3429e-002	2.7108e-002	1.3653e-002	6.8512e-003	3.4318e-003
		0.9789	0.9895	0.9948	0.9974	0.9987
2^{-12}		5.3723e-002	2.7268e-002	1.3735e-002	6.8929e-002	3.4529e-003
		0.9784	0.9893	0.9947	0.9973	0.9987
2^{-14}		1.5475e-001	1.6134e-001	7.8680e-002	2.5410e-002	6.6458e-002
		-0.0602	1.0360	1.6306	1.9348	1.9406
2^{-16}		1.7530e-001	2.6093e-001	2.6474e-001	1.6807e-001	7.8391e-002
		-0.5739	-0.0209	0.6555	1.1003	1.5661
2^{-18}		1.7554e-001	2.6692e-001	3.0979e-001	3.0140e-001	2.6136 e-001
		-0.6046	-0.2149	0.0396	0.2056	0.5956
2^{-20}		1.7554e-001	2.6693e-001	3.1039e-001	3.1017e-001	3.0689e-001
		-0.6047	-0.2176	0.0010	0.0154	0.0344

Table 2: The maximum point wise errors and numerical rates of convergence for Example 3.1 with $\epsilon = 0.01$ and various values of δ.

	$M \rightarrow$	64	128	256	512	1024
$\delta \downarrow$	$N \rightarrow$	100	200	300	400	500
0.02		1.0568e-002	5.3136e-003	3.5540e-003	2.6683e-003	2.1355e-003
		0.9919	0.9958	0.9981	0.9988	0.9991
0.04		1.0750e-002	5.4056e-003	3.6156e-003	2.7146e-003	2.1725e-003
		0.9918	0.9958	0.9981	0.9988	0.9991
0.06		1.0934e-002	5.4985e-003	3.6779e-003	2.7614e-003	2.2100e-003
		0.9916	0.9957	0.9981	0.9988	0.9991
0.08		1.1120e-002	5.5925e-003	3.7409e-003	2.8087e-003	2.2479e-003
		0.9916	0.9957	0.9980	0.9988	0.9991
0.10		1.1309e-002	5.6876e-003	3.8047e-003	2.8567e-003	2.2862e-003
		0.9916	0.9957	0.9980	0.9988	0.9991

Table 3: The maximum point wise errors calculated using the numerical scheme presented in Section 2.2 for Example 3.1 for $\delta = 0.5\epsilon$.

$\epsilon = 2^{-10}$	$N = 64$	$N = 128$	$N = 256$	$N = 512$	$N = 1024$
$M = 64$	5.5836e-002 ($\lambda = 128$)	1.3814e-001 ($\lambda = 64$)	3.1104e-001 ($\lambda = 32$)	3.1104e-001 ($\lambda = 16$)	3.1104e-001 ($\lambda = 8$)
$M = 128$	1.7022e-002 ($\lambda = 512$)	1.3885e-001 ($\lambda = 256$)	2.3876e-001 ($\lambda = 128$)	2.3876e-001 ($\lambda = 64$)	2.3876e-001 ($\lambda = 32$)
$M = 256$	1.7037e-002 ($\lambda = 2048$)	5.7204e-002 ($\lambda = 1024$)	5.7204e-002 ($\lambda = 512$)	5.7204e-002 ($\lambda = 256$)	5.7204e-002 ($\lambda = 128$)
$M = 512$	1.7038e-002 ($\lambda = 8192$)	4.7301e-003 ($\lambda = 4096$)	4.7301e-003 ($\lambda = 2048$)	4.7301e-003 ($\lambda = 1024$)	4.7301e-003 ($\lambda = 512$)
$M = 1024$	1.7039e-002 ($\lambda = 32768$)	8.5570e-003 ($\lambda = 16384$)	1.0729e-003 ($\lambda = 8192$)	1.0729e-003 ($\lambda = 4096$)	1.0729e-003 ($\lambda = 2048$)

Table 4: The maximum point wise errors calculated using the numerical scheme presented in Section 2.4 for Example 3.1 for $\delta = 2^{-5}$.

$\epsilon = 2^{-10}$	$N = 64$	$N = 128$	$N = 256$	$N = 512$	$N = 1024$
$M = 64$	5.3284e-002 ($\lambda = 128$)	1.3717e-001 ($\lambda = 64$)	2.3593e-001 ($\lambda = 32$)	2.9992e-001 ($\lambda = 16$)	3.1609e-001 ($\lambda = 8$)
$M = 128$	1.7513e-002 ($\lambda = 512$)	1.5652e-002 ($\lambda = 256$)	5.6836e-002 ($\lambda = 128$)	2.4239e-001 ($\lambda = 64$)	2.4239e-001 ($\lambda = 32$)
$M = 256$	1.7528e-002 ($\lambda = 2048$)	8.7994e-003 ($\lambda = 1024$)	1.7818e-002 ($\lambda = 512$)	5.8077e-002 ($\lambda = 256$)	5.8077e-002 ($\lambda = 128$)
$M = 512$	1.7530e-002 ($\lambda = 8192$)	4.4106e-003 ($\lambda = 4096$)	4.7897e-003 ($\lambda = 2048$)	4.7897e-003 ($\lambda = 1024$)	4.7897e-003 ($\lambda = 512$)
$M = 1024$	1.7530e-002 ($\lambda = 32768$)	1.1038e-003 ($\lambda = 16384$)	1.1038e-003 ($\lambda = 8192$)	1.1038e-003 ($\lambda = 4096$)	1.1038e-003 ($\lambda = 2048$)

the effect of small shift on the boundary layer behavior of the solution. The maximum absolute errors are tabulated in the form of Table 3 for $\epsilon = 2^{-10}$, $\delta = 0.5\epsilon$ for various values of $\lambda = \Delta t/h^2$. It can be observed from this table that irrespective for the value of λ, the maximum absolute error remains the same, which demonstrates the unconditional stability of the finite difference scheme described in Section 2.1. The maximum absolute errors are tabulated in the form of Table 4 for $\epsilon = 2^{-10}$, $\delta = 2^{-5}$ for various values of $\lambda = \Delta t/h^2$. It can be observed from this table that irrespective of the value of λ, the maximum absolute error remains the same, which demonstrates the unconditional stability of the finite difference scheme in Section 2.4.

Example 3.2. For

$$\frac{\partial u(x,t)}{\partial t} - \epsilon \frac{\partial^2 u(x,t)}{\partial x^2} + 2e^{-1}u(x,t-\delta) = 0,$$
$$(x,t) \in D : \{0 < x < 1, 0 < t \leq 2\},$$

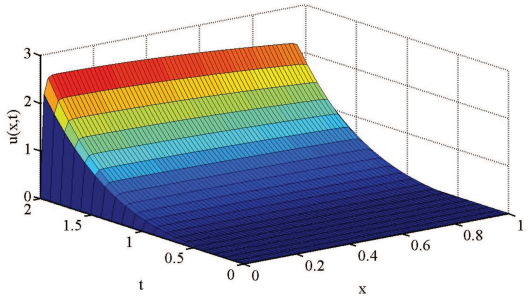

Figure 1: Numerical Solution $U(x,t)$ of Example 3.1 with $\epsilon = 2^{-20}$, $\delta = 0.5\epsilon$.

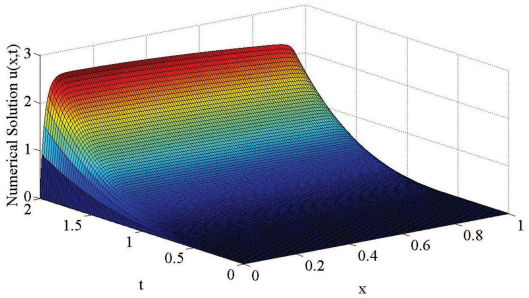

Figure 2: Numerical Solution $u(x,t)$ of Example 3.1 with $\epsilon = 2^{-10}$, $\delta = 0.06$.

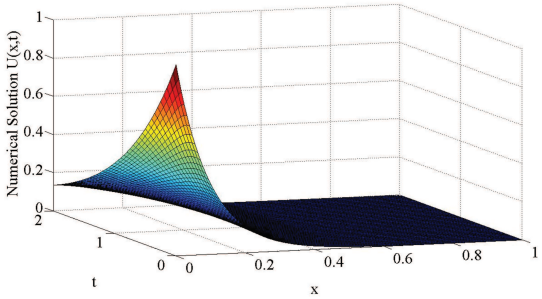

Figure 3: Numerical Solution $U(x,t)$ of Example 3.2 with $\epsilon = 0.01$, $\delta = 0.5\epsilon$.

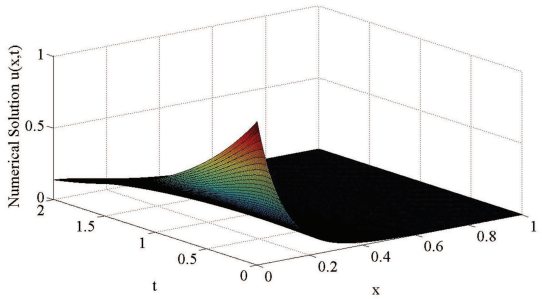

Figure 4: Numerical Solution $u(x,t)$ of Example 3.2 with $\epsilon = 0.01$, $\delta = 0.06$.

Table 5: The maximum point wise errors and numerical rates of convergence for Example 3.2 with $\delta = 0.5\epsilon$.

$\epsilon \downarrow$ $M \rightarrow$ / $N \rightarrow$	64	128	256	512	1024
	20	40	80	160	320
2^{-1}	3.8685e-003	2.8641e-003	1.8608e-003	1.0827e-003	5.9943e-004
	0.4337	0.6221	0.7814	0.8529	0.9252
2^{-2}	4.7975e-003	3.1217e-003	1.8170e-003	1.0038e-003	5.2781e-004
	0.6199	0.7807	0.8561	0.9274	0.9635
2^{-4}	4.6765e-003	2.6929e-003	1.4873e-003	8.0139e-004	4.2284e-004
	0.7963	0.8565	0.8921	0.9224	0.9454
2^{-6}	4.4829e-003	2.6268e-003	1.4767e-003	7.9891e-004	4.2154e-004
	0.7711	0.8309	0.8863	0.9224	0.9457
2^{-8}	4.3306e-003	2.6158e-003	1.4737e-003	7.9798e-004	4.2087e-004
	0.7273	0.8278	0.8850	0.9230	0.9449
2^{-10}	3.6039e-003	2.4568e-003	1.4433e-003	7.8909e-004	4.1966e-004
	0.5528	0.7674	0.8711	0.9110	0.9427
2^{-12}	1.0282e-002	2.7064e-003	1.1090e-003	7.1493e-003	4.0251e-004
	1.9257	1.2871	0.6334	0.8288	0.9054
2^{-14}	5.4376e-002	2.8248e-002	1.1411e-002	3.5324e-003	9.2016e-004
	0.9448	1.3077	1.6918	1.9407	2.1682
2^{-16}	9.2557e-002	7.5817e-002	5.3803e-002	2.9540e-002	1.2014e-002
	0.2878	0.4949	0.8650	1.2980	1.6463
2^{-18}	1.0979e-001	1.1174e-001	9.1303e-002	7.7166e-002	5.4832e-002
	-0.0254	0.2915	0.2427	0.4930	0.8691
2^{-20}	1.1262e-001	1.3012e-001	1.2648e-001	1.0610e-001	9.4454e-002
	-0.2084	0.0410	0.2536	0.1677	0.2700

with the initial data $u(x,t) = e^{-(t+x/\sqrt{\epsilon})}$, $(x,t) \in D_1 : \{0 \le x \le 1, -\delta \le t \le 0\}$ and the boundary conditions $u(0,t) = e^{-t}$ and $u(1,t) = e^{-(t+1/\sqrt{\epsilon})}$, $t \in (0,2]$.

The maximum absolute errors are tabulated in the form of Table 5 for $\delta = 0.5\epsilon$ and various values of ϵ. The graph of the solution for $\epsilon = 0.01$ and $\delta = 0.5\epsilon$ is plotted in Fig. 3 to examine the effect of small shift on the boundary layer behavior of the solution. The maximum absolute errors for $\delta = 0.06$ and for various values of ϵ are tabulated in Table 6. The graph of the solution for $\epsilon = 0.01$ and $\delta = 0.06$ is plotted in Fig. 4 to examine the effect of small shift on the boundary layer behavior of the solution. The maximum absolute errors are tabulated in the form of Table 7 for $\epsilon = 2^{-10}$, $\delta = 0.5\epsilon$, for various values of $\lambda = \Delta t/h^2$. It can be observed from this table that irrespective of the value of λ, the maximum absolute error remains the same, which demonstrates the unconditional stability of the finite difference scheme described in Section 2.2. The maximum absolute errors are tabulated in the form of Table 8 for $\epsilon = 2^{-10}$, $\delta = 2^{-5}$, for various values of $\lambda = \Delta t/h^2$. It can be observed from this table that irrespective of the value of λ, the maximum absolute error remains the same, which demonstrates the unconditional stability of the finite difference scheme described in Section 2.4.

Table 6: The maximum point wise errors and numerical rates of convergence for Example 3.2 with $\delta = 0.06$.

$\epsilon \downarrow$	$M \rightarrow$ / $N \rightarrow$	64 / 100	128 / 200	256 / 300	512 / 400	1024 / 500
2^{-1}		1.4598e-003	8.2153e-004	5.7013e-004	4.3759e-004	3.5454e-004
		0.8294	0.9088	0.9358	0.9532	0.9617
2^{-2}		1.4624e-003	7.8360e-004	5.3591e-004	4.0668e-004	3.2786e-004
		0.9001	0.9463	0.9651	0.9730	0.9788
2^{-4}		1.1617e-003	6.1243e-004	4.1749e-004	3.1973e-004	2.5951e-004
		0.9236	0.9381	0.9338	0.9419	0.9477
2^{-6}		1.1079e-003	6.0056e-004	4.1583e-004	3.1963e-004	2.5950e-004
		0.8834	0.9168	0.9292	0.9416	0.9477
2^{-8}		1.1178e-003	5.0039e-004	4.0275e-004	3.1811e-004	2.5915e-004
		1.1595	0.7440	0.9015	0.9371	0.9460
2^{-10}		1.6053e-002	5.4889e-003	7.9227e-004	2.9877e-004	2.5708e-004
		1.5483	1.8240	2.0742	0.8823	0.9393
2^{-12}		6.1932e-002	3.7513e-002	1.1003e-002	1.5502e-002	2.3276e-004
		0.7233	1.1484	1.6655	2.0117	0.8518
2^{-14}		9.4838e-002	8.3589e-002	5.2928e-002	1.6924e-002	2.4488e-003
		0.1821	0.3879	0.8989	1.5437	1.9208
2^{-16}		1.2958e-001	1.1228e-001	9.3348e-002	6.3881e-002	2.2801e-002
		0.2067	0.1500	0.2705	0.7308	1.4343
2^{-18}		1.4836e-001	1.3945e-001	1.2174e-001	1.0119e-001	7.1655e-002
		0.0893	0.1313	0.1376	0.2467	0.6098
2^{-20}		1.5157e-001	1.5816e-001	1.4307e-001	1.2732e-001	1.0663e-001
		-0.0614	0.1282	0.0968	0.1301	0.2194

Table 7: The maximum point wise errors calculated using the numerical scheme presented in Section 2.2 for Example 3.2 for $\delta = 0.5\epsilon$.

$\epsilon = 2^{-10}$	$N = 64$	$N = 128$	$N = 256$	$N = 512$	$N = 1024$
$M = 64$	7.6839e-003	2.2629e-002	9.1164e-002	9.1164e-002	9.1164e-002
	($\lambda = 128$)	($\lambda = 64$)	($\lambda = 32$)	($\lambda = 16$)	($\lambda = 8$)
$M = 128$	1.4518e-003	2.3104e-002	4.7080e-002	4.7080e-002	4.7080e-002
	($\lambda = 512$)	($\lambda = 256$)	($\lambda = 128$)	($\lambda = 64$)	($\lambda = 32$)
$M = 256$	1.7569e-003	8.5972e-003	8.5972e-003	8.5972e-003	8.5972e-003
	($\lambda = 2048$)	($\lambda = 1024$)	($\lambda = 512$)	($\lambda = 256$)	($\lambda = 128$)
$M = 512$	1.7823e-003	6.6720e-004	6.6720e-004	6.6720e-004	6.6720e-004
	($\lambda = 8192$)	($\lambda = 4096$)	($\lambda = 2048$)	($\lambda = 1024$)	($\lambda = 512$)
$M = 1024$	1.7896e-003	9.7468e-004	5.1675e-004	2.6755e-004	1.3263e-004
	($\lambda = 32768$)	($\lambda = 16384$)	($\lambda = 8192$)	($\lambda = 4096$)	($\lambda = 2048$)

Table 8: The maximum point wise errors calculated using the numerical scheme presented in Section 2.4 for Example 3.2 for $\delta = 2^{-5}$.

$\epsilon = 2^{-10}$	$N = 64$	$N = 128$	$N = 256$	$N = 512$	$N = 1024$
$M = 64$	2.7128e-003 ($\lambda = 128$)	6.4549e-003 ($\lambda = 64$)	3.8367e-002 ($\lambda = 32$)	3.8367e-002 ($\lambda = 16$)	3.8367e-002 ($\lambda = 8$)
$M = 128$	8.8630e-004 ($\lambda = 512$)	1.4203e-002 ($\lambda = 256$)	1.4203e-002 ($\lambda = 128$)	1.4203e-002 ($\lambda = 64$)	1.4203e-002 ($\lambda = 32$)
$M = 256$	9.1492e-004 ($\lambda = 2048$)	2.2697e-003 ($\lambda = 1024$)	2.2697e-003 ($\lambda = 512$)	2.2697e-003 ($\lambda = 256$)	2.2697e-003 ($\lambda = 128$)
$M = 512$	9.1915e-004 ($\lambda = 8192$)	2.2848e-004 ($\lambda = 4096$)	2.2848e-004 ($\lambda = 2048$)	2.2848e-004 ($\lambda = 1024$)	2.2848e-004 ($\lambda = 512$)
$M = 1024$	9.1942e-004 ($\lambda = 32768$)	2.3180e-004 ($\lambda = 16384$)	2.3180e-004 ($\lambda = 8192$)	2.3180e-004 ($\lambda = 4096$)	2.3180e-004 ($\lambda = 2048$)

4. Conclusions

In this paper, we presented exponentially fitted finite difference methods for a class of singularly perturbed one-dimensional parabolic partial differential equations with a small negative shift in the temporal variable. The numerical results presented in Tables 1-2, 5-6 show the high accuracy and convergence of the proposed finite difference methods. Tables 3-4, 7-8 demonstrate the unconditional stability of the proposed finite difference methods. Figs. 1-4 demonstrate the effect of the shift parameter on the boundary layer behavior of the solution of the problem. From the numerical results it is concluded that the presented methods offer significant advantage for the linear singularly perturbed parabolic partial differential equations with a small negative shift.

Acknowledgments The authors wish to thank the Department of Science & Technology, Government of India, for their financial support under the project No. SR/S4/MS: 598/09. Authors are grateful to the referees for their valuable suggestions and comments.

References

[1] J. Wu, Theory and Applications of Partial Functional Differential Equations, Springer, NewYork, 1996.

[2] M. Musila and P. Lánský, *Generalized Steiń s model for anatomically complex neurons*, Biosystems, 25 (1991), pp. 179–191.

[3] O. Arino, M. L. Hbid and E. Ait Dads, Delay Differential Equations and Applications, Springer, Berlin,2006.

[4] A. Friedman, Partial Differential Equations of Parabolic Type, Prentice-Hall, Englewood Cliffs, 1964.

[5] J. D. Murray, Mathematical Biology I: An Introduction, third edition, Springer-Verlag, Berlin, 2001.

[6] J. B. Buriea, A. Calonnec and A. Ducrot, *Singular perturbation analysis of travelling waves for a model in Phytopathology*, Math. Modell. Natural Phenomena, 1(1) (2006), pp. 49–62.

[7] A. R. Ansari and A. F. Hegarty, *A note on iterative methods for solving singularly perturbed problems using non-monotone methods on Shishkin meshes*, Comput. Methods Appl. Mech. Eng., 192 (2003), pp. 3673–3687.
[8] A. R. Ansari, A. F. Hegarty and G. I. Shishkin, *A note on fitted operator methods for the classical laminar free jet problem*, Appl. Numer. Math., 45 (2003), pp. 353–365.
[9] A. R. Ansari and A. F. Hegarty, *Numerical solution of a convection diffusion problem with Robin boundary conditions*, J. Comput. Appl. Math., 156 (2003), pp. 221–238.
[10] C. Clavero, J. C. Jorge, F. Lisbona and G. I. Shishkin, *An alternating direction scheme on a nonuniform mesh for reaction-diffusion parabolic problem*, IMA J. Numer. Anal., 20 (2000), pp. 263–280.
[11] H. G. Roos, M. Stynes and L. Tobiska, Numerical Methods for Singularly Perturbed Differential Equations, Convection-Diffusion and Flow Problems, Springer Series in Computational Mathematics, 24, Springer, Berlin, 1996.
[12] J. J. H. Miller, E. ÓRiordan and G. I. Shishkin, Fitted Numerical Methods for Singular Perturbation Problems, Error Estimate in the Maximum Norm for Linear Problems in One and Two Dimensions, World Scientific, Singapore, 1996.
[13] P. A. Farrell, A. F. Hegarty, J. J. H. Miller, E. ÓRiordan and G. I. Shishkin, Robust Computational Techniques for Boundary Layers, Chapman & Hall, London, 2000.
[14] P. W. Hemker, G. I. Shishkin and L. P. Shishkina, *Novel defect-correction high-order in space and time accurate schemes for parabolic singularly perturbed convection-diffusion problems*, Comput. Methods Appl. Math., 3 (2003), pp. 387–404.
[15] P. W. Hemker, G. I. Shishkin and L. P. Shishkina, *The use of defect correction for the solution of parabolic singular perturbation problems*, Z. Angew. Math. Mech., 76 (1997), pp. 59–74.
[16] P. W. Hemker, G. I. Shishkin and L. P. Shishkina, *ε-uniform schemes with high-order time-accuracy for parabolic singular perturbation problems*, IMA J. Numer. Anal., 20 (2000), pp. 99–121.
[17] G. I. Shishkin, *Robust novel high-order accurate numerical methods for singularly perturbed convection-diffusion problems*, Math. Model. Anal., 10 (2005), pp. 393–412.
[18] A. R. Ansari, S. A. Bakr and G. I. Shishkin, *A parameter-robust finite difference method for singularly perturbed delay parabolic partial differential equations*, J. Comput. Appl. Math., 205 (2007), pp. 552–566.
[19] Y. Wang, *An efficient computational method for a class of singularly perturbed delay parabolic partial differential equation*, Int. J. Comput. Math., 88(16) (2011), pp. 3496–3506.
[20] E. B. M. Bashier and K. C. Patidar, *A novel fitted operator finite difference method for a singularly perturbed delay parabolic partial differential equation*, Appl. Math. Comput., 217 (2011), pp. 4728–4739.
[21] H. Tian, Numerical Treatment of Singularly Perturbed Delay Differential Equations, Ph.D. thesis, University of Manchester, 2000.
[22] E. P. Doolan, J. J. H. Miller and W. H. A. Schilders, Uniform Numerical Methods for Problems with Initial and Boundary Layers, Doole Press, Dublin, 1980.
[23] G. D. Smith, Numerical Solution of Partial Differential Equations: Finite Difference Methods, Clarendon Press, Oxford, 1985.